Philippine e-Journal for Applied Research and Development 8(2018), 1-14 ISSN 2449-3694 (Online)
http://pejard.slu.edu.ph/vol.8/2018.06.30.pdf

Modelling of Amorphous Silicon Thin-Film Photovoltaic Module Performance Using Current-Voltage Characteristics

Adrian Augusto M. Sumalde[1,*] and Miguel T. Escoto Jr.[2]

[1]Department of Electrical Engineering, College of Engineering and Agro-Industrial Technology, University of the Philippines - Los Baños; [2]Institute of Electrical and Electronics Engineering, University of the Philippines - Diliman
** Corresponding author (aamsumalde@gmail.com)*

Received, 28 March 2018; Accepted, 22 June 2018; Published, 30 June 2018

Abstract

Amorphous silicon thin-film photovoltaic modules have been developed as potential alternatives to crystalline-based due to their relatively less cost of production. This study incorporated both field measurements and software-based solutions to develop current-voltage characteristics of a SF100 a-Si thin film module as well as the mathematical functions of its electrical quantities with four environmental variables: irradiance, front panel temperature, back panel temperature, and ambient temperature. Results include twenty current-voltage curves based on the two-term exponential model with R^2 scores greater than 90%, and equations for maximum power, fill factor, and efficiency obtained from factor analysis. The maximum power equation illustrates that the module's output power is heavily influenced by the backside temperature, front/surface temperature, and irradiance, as compared to ambient temperature.

Keywords: solar photovoltaic modules, current-voltage efficiency, irradiance, temperature

Introduction

Solar photovoltaic (PV) technology has steadily been developed in order to harness energy from sunlight. Most solar PV modules in the market are made from crystalline silicon. However, there are emerging thin-film technologies based on many different materials like copper indium diselenide (CIS), cadmium telluride (CdTe), and cadmium sulfide (CdS). Amorphous silicon (a-Si), a glassy alloy of silicon and hydrogen, is also a popular choice for thin-film solar cells [1]. Amorphous silicon thin film modules have lower efficiencies (7-9%) than their crystalline silicon counterparts (up to 22%), but they are considered due to their decreased production costs [1, 2].

In general, two broad approaches are used to evaluate the performance of PV modules, either by modelling and simulation or through field measurements. Simulations are often carried out using systems software such as MATLAB-Simulink [3] and LabVIEW [4], as well as through lab-developed methods such as PHANTASM (PHotovoltaic ANalysis and TrAnsient Simulation Method) [5].

Simulation approaches often make use of two major conditions, the Standard Test Conditions (STC) and the Nominal Operating Cell Temperature (NOTC). STC is specified at an irradiance of 1000 W/m^2, 25^{o}C cell temperature, and 1.5 global air mass (AM) [6], while NOTC is measured at the "nominal terrestrial environment" characterized by an irradiance

of 800 W/m^2, average wind speed of 1 m/s, and panel orientation in open rack mounting [5, 7].

Simulations in previous work were done through a PV module based on its equivalent circuit model. In terms of characterization, the current-voltage (I-V) characteristics of the PV module are used to locate and identify electrical parameters such as open-circuit voltage (V_{oc}), short-circuit current (I_{sc}), and maximum power (P_{max}) [8, 9]. These equations are often derived from three equivalent solar cell models, namely: (1) ideal model, (2) single-diode model, and (3) double-diode model [8]. Equations derived from these models reveal that the PV cell (and, by extension, module) output current can be represented using various combinations of exponential functions stemming from the behaviour of a semiconductor diode's current. Other studies have also attempted to represent PV module models in terms of rational equations [10] and piecewise equations [11] based on the maximum power point of the I-V curve, in pursuit of less complicated calculations and number of required points.

From these simulations, general trends describing the effects of irradiance and cell/surface temperature and have been established and verified. First, since a PV module's operation is founded on the photovoltaic effect, a PV module's output current – and consequently, output power – is directly proportional to the incident irradiance [12, 13, 2]. Second, the cell operating temperature has been found to reduce the performance of a PV module, specifically, by decreasing its output voltage and consequently the output power and efficiency [14].

Field-based measurements have also been researched not only to verify existing relationships between parameters, but as well as to explore novel trends in PV module behavior. For instance, the PV module's backside temperature [15, 16] and ambient temperature [17] have also been investigated. In particular, there has been a case where the backside temperature of crystalline modules was found to be up to 3^{o}C higher than the cell temperature itself [18]. Similar to the surface temperature, an increase in the panel's backside temperature reduces the performance; however, reduced backside temperatures have been found to offset the loss as initially projected based on surface temperatures alone [15]. Ambient temperature has also been found to have a positive effect on the output of a PV module [19]; however, it has not been the subject of much study as compared to a cell's surface temperature.

This study combines the aspects of field-based measurements with the aid of mathematical methods in order to pursue the following objectives: (1) model I-V characteristic curves for a-Si PV modules exposed to varying irradiance and temperature; (2) verify the I-V characteristic curves based on existing PV trends, and (3) develop mathematical models for output power, fill factor, and efficiency as a function of irradiance (G), front panel temperature (T_F), panel backside temperature (T_B), and ambient temperature (T_A).

Methodology

Experimental Setup

One hundred-Watt SF100 model thin-film a-Si panels (see Table 1 for physical and electrical parameters) were obtained and tilted at an angle of 14.14^o with respect to the horizontal, matching the latitude of the University of the Philippines – Los Baños, where the set-up was made.

Table 1. Physical and electrical parameters of SF100 model a-Si PV module.

Parameter	**Value**
Dimensions (mm)	1414 x 1114 x 35 mm
Weight (kg)	20.3 kg
Maximum power at STC	100 W
Maximum power voltage (V_{mp}), STC	77 V
Maximum power current (I_{mp}), STC	1.35 A
Open-circuit voltage, STC	99 V
Short-circuit current, STC	1.65 A
Effective solar area, m^2	1.421 m^2
Efficiency, STC	7%

Irradiance was measured using a LI-COR LI-200SA pyranometer sensor. This pyranometer

incorporates a silicon photodiode as its sensing element, and has a spectral response of 0.4 to 1.2 µm, covering the sunlight wavelength range. The recorded irradiance has a unit of Watts per square meter (W/m^2).

Temperature measurements were obtained using Type J (iron-constantan) thermocouple wires connected to a Campbell CR850 datalogger. With a range of -40 to 750 degrees C, the expected temperature measurements are well covered by the selected thermocouples. Two of the thermocouple wires are attached to the front and back surfaces of the PV module, while the third one is kept under shelter for ambient temperature measurements. A B&K programmable DC electronic load model BK850 was used as the variable load for the PV modules.

The block diagram summarizing the connections of the equipment is shown in Figure 1.

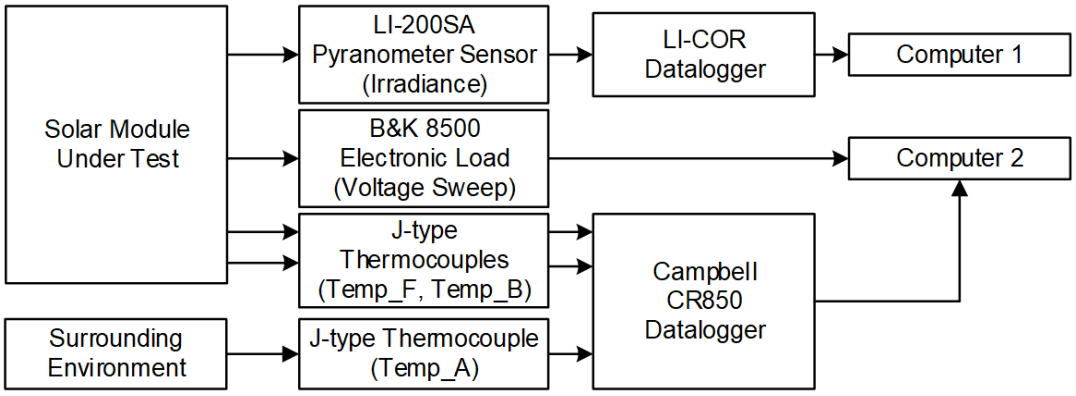

Figure 1. Block diagram of equipment connections.

Data Acquisition

The LI-COR datalogger's log routine was programmed to record samples every five seconds, before averaging it per minute (i.e., average of 12 samples for each data). The same recording metric was programmed for the temperature measurements.

The electronic load was programmed to operate in constant-voltage (CV) sweep. In order to match the desired per-minute timing, the voltage range (0 to open-circuit voltage) was divided into intervals of 0.4125 Volt each. This allowed one full CV sweep to be completed in four minutes. During the course of the voltage sweep, the electronic load would return the current instantly from short to open circuit condition. These current-voltage points formed the I-V characteristic curves for the two types of solar PV modules. It must be noted that the sweep may terminate before the rated open-circuit voltage of 99 Volts; the DC electronic load automatically stops once the reading for the current reaches 0 Amperes.

Per-minute recording was then done, with the timestamps of the voltage sweeps matching the environmental data collection. Data was collected and grouped based on four desired irradiance levels: 0.25 sun (250 W/m^2), 0.5 sun (500 W/m^2), 0.75 sun (750 W/m^2) and 1 sun (1000 W/m^2), with a 10% irradiance allowance.

I-V Curve Development

For each irradiance level, five complete I-V curves were developed for a total of 20 I-V curves. Each curve was then processed for curve fitting tool using MATLAB R2012b. This study used a two-term exponential fit following the general model *Exp2* that was based from two-diode circuit model equivalent, with exponential terms as well. The resulting fitted equations are of the

form

$$I(v) = a * \exp(b * v) + c * \exp(d * v)$$

Equation 1

Where *i and v* are the current and voltage for each point, while *a, b, c,* and *d* are the constants obtained from the curve fitting tool. Each fit equation was ensured to have R^2 value of at least 90% for goodness-of-fit.

Electrical Parameter Calculation

The values obtained from the fitted curves for each irradiance were then used to determine the following electrical parameters: (1) maximum power output, (2) fill factor, and (3) maximum efficiency.

For each fitted curve, the intercepts of each I-V equation gives a corresponding short-circuit current, I_{SC}, and open-circuit voltage, V_{OC}. The output power of the module is the product of the voltage and current, with the maximum value over the entire curve being noted as the maximum power point. The voltage and current at this maximum power were also taken and used to compute for the fill factor using the following equation [13]:

$$FF = \frac{I_{mp}V_{mp}}{I_{SC}V_{OC}}$$

Equation 2

Where I_{mp} and V_{mp} are the voltage and current at the maximum power point, while I_{SC} and V_{OC} are the short-circuit current and the open-circuit voltage as described above. For efficiency, the ratio of the output and the input power was calculated, as the input power being the product of irradiance, G, and the PV module's effective surface area [20]. The maximum value of this efficiency is taken for analysis:

$$\eta = \frac{P_{\max}}{G \cdot A_{effective}}$$

Equation 3

With 20 I-V curves obtained, 20 points each for the three electrical parameters are available. These values were then subjected to statistical analysis for model development.

Development of Mathematical Models

The current-voltage data points generated from the 20 I-V curves developed from MATLAB's curve fitting tool are then used for the development of the statistical model, using regression analysis. As one of the study's aims is to develop a mathematical equation in terms of four variables, it was necessary to determine if any existing relationship between these independent variables exists. Specifically, it is perceived that as the irradiance increases, the temperature at the surface, back, and ambient would also increase; it is also believed that the increase in these three temperatures are not independent of each other and would be correlated in some manner.

This necessitated the application of Pearson's correlation (*r*-statistic) to check for multicollinearity. As multicollinearity was proven, factor analysis was performed in this study to allow for proper representation of the contribution (termed 'loading') of each independent variable to the dependent variable, and assigning one single 'factor' as the representative of all independent variables and their corresponding factors [21].

The resulting electrical models for maximum power, efficiency, and fill factor thus follow the equation form shown below:

$$f(T_F, T_B, T_A, G) = \beta_o + \beta_1(l_1T_A + l_2T_B + l_3T_A + l_4G)$$

Equation 4

Where T_F, T_B, T_A, and G are the front, back, and ambient temperatures, and irradiance, respectively; β_0 and β_1 are the intercept and slope of the derived model, and l_1 to l_4 are the loadings of the four independent parameters T_F, T_B, T_A, and G.

Statistical tests were done using SAS software version 9.3 and STATA Statistical Software version 12.

Results and Discussion

I-V Curve Development and Electrical Parameter Calculations

The equations derived from the Curve Fitting Tool for all 20 I-V curves and the average for each sun level are presented in Table 2. Each curve exhibits the behaviour of the I-V characteristics in the form of Equation 1, while the R^2 supports the validity of the two-term exponential equations modelled.

Table 2. Fitted I-V curves of a-Si PV modules for varying irradiance levels

#	Curve Label	Two-term exponential fit equation	R^2
1	TF_0.25_Exp1	i(v) = -0.025*exp(0.05899v) + 0.4801*exp(0.0005123v)	0.9804
2	TF_0.25_Exp2	i(v) = -2.981e-06*exp(0.1367v) + 0.3931*exp(1.155e-06v)	0.9495
3	TF_0.25_Exp3	i(v) = -6.633e-05*exp(0.1002v) + 0.4103*exp(-0.001782v)	0.9693
4	TF_0.25_Exp4	i(v) = -2.418e-07*exp(0.1589v) + 0.2473*exp(-0.002328v)	0.967
5	TF_0.25_Exp5	i(v) = -4.209e-12*exp(0.2721v) + 0.4153*exp(-0.003408v)	0.946
6	TF_0.5_Exp1	i(v) = -9.871e-05*exp(0.09863v) + 0.8455*exp(-0.0009266v)	0.9977
7	TF_0.5_Exp2	i(v) = -8.19e-06*exp(0.1213v) + 0.6576*exp(-0.001901v)	0.977
8	TF_0.5_Exp3	i(v) = -0.0001561*exp(0.09406v) + 0.8746*exp(-0.0008052v)	0.9988
9	TF_0.5_Exp4	i(v) = -0.0002251*exp(0.08974v) + 0.8738*exp(-0.0008963v)	0.9924
10	TF_0.5_Exp5	i(v) = -0.0002369*exp(0.08705v) + 0.7014*exp(-0.00001189v)	0.9708
11	TF_0.75_Exp1	i(v) = -6.011e-05*exp(0.1084v) + 1.193* exp(-0.002117v)	0.9971
12	TF_0.75_Exp2	i(v) = -0.0002114*exp(0.0951v) + 1.073*exp(0.0000263v)	0.9988
13	TF_0.75_Exp3	i(v) = -0.0002988*exp(0.09293v) + 1.213*exp(-0.002125v)	0.9704
14	TF_0.75_Exp4	i(v) = -5.943e-05*exp(0.1084v) + 1.19*exp(-0.002125v)	0.9966
15	TF_0.75_Exp5	i(v) = -5.854e-05*exp(0.1089v) + 1.176*exp(-0.001777v)	0.9934
16	TF_1_Exp1	i(v) = -0.00106*exp(0.08215v) + 1.753*exp(-0.001539v)	0.9988
17	TF_1_Exp2	i(v) = -0.001987*exp(0.07321v) + 1.478*exp(0.000561v)	0.9972
18	TF_1_Exp3	i(v) = -0.0008618*exp(0.08506v) + 1.703*exp(-0.0007205v)	0.9998
19	TF_1_Exp4	i(v) = -0.0004703*exp(0.09206v) + 1.728*exp(-0.00121v)	0.9993
20	TF_1_Exp5	i(v) = -0.001347*exp(0.08051v) + 1.778*exp(-0.0007872v)	0.9997
21	TF_0.25_Ave	i(v) = -0.0003331*exp(0.07722v) + 0.3856*exp(-0.0007206v)	0.9937
22	TF_0.5_Ave	i(v) = -0.0001275*exp(0.09465v) + 0.7879*exp(-0.0008319v)	0.9944
23	TF_0.75_Ave	i(v) = -0.0001493*exp(0.09867v) + 1.168*exp(-0.00167v)	0.99
24	TF_1_Ave	i(v) = -0.00346*exp(0.06876v) + 1.675*exp(-0.00004077v)	0.9872

For each curve, the voltage and current intercepts represent the open-circuit voltage and short-circuit current; the point of concavity represents the maximum power point of the curve, where the voltage and current at that point are also used to calculate for fill factor and efficiency using Equations 2 and 3.

Tables 3 and 4 summarize the environmental and electrical parameters calculated from the models for 0.25 Sun.

The values from Tables 3 and 4 provide explanation to Figure 2. Curve 4 has evident reduced performance due to the effects of the increased front and back temperatures, which offset the irradiance – already at low sun to begin with. On the other hand, the combination of a higher irradiance and a lower set of temperatures supports the improved output of Curve 1.

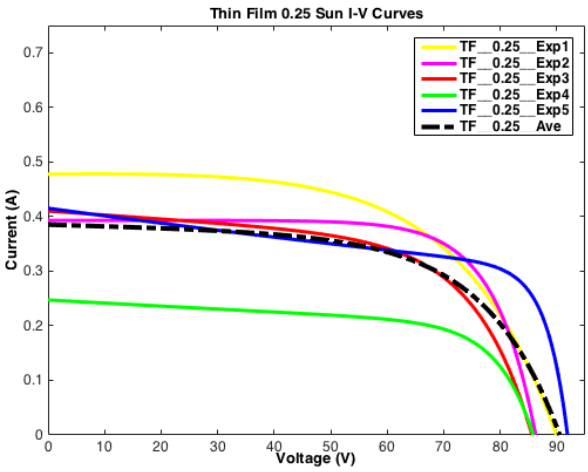

Figure 2. I-V curves at 0.25 sun.

Table 3. Environmental quantities at each 0.25 Sun I-V curve.

#	Curve Label	G_{ave} (W/m^2)	$T_{F(ave)}$ (°C)	$T_{B(ave)}$ (°C)	$T_{A(ave)}$ (°C)
1	TF_0.25_Exp1	262.628	31.2233	30.0475	27.4673
2	TF_0.25_Exp2	243.322	30.4771	29.7043	27.2009
3	TF_0.25_Exp3	240.029	30.8929	29.2529	27.9200
4	TF_0.25_Exp4	256.66	34.237	33.207	31.1211
5	TF_0.25_Exp5	237.9	31.8627	30.5878	28.8778

Table 4. Electrical quantities at each 0.25 Sun I-V curve.

#	Curve Label	P_{max} (W)	V_{MP} (V)	I_{MP} (A)	V_{OC} (V)	I_{SC} (A)	FF	η (%)
1	TF_0.25_Exp1	24.7728	63.9375	0.3875	89.9095	0.4776	0.5769	6.6381
2	TF_0.25_Exp2	24.5571	68.8875	0.3565	86.2448	0.3931	0.7243	7.1023
3	TF_0.25_Exp3	20.8493	64.7625	0.3219	85.6034	0.4102	0.5938	6.1127
4	TF_0.25_Exp4	13.5694	69.3	0.1958	85.8288	0.2473	0.6392	3.7206
5	TF_0.25_Exp5	24.3492	79.6125	0.3058	91.885	0.4153	0.6381	7.2027

In general, the obtained quantities at 0.25 sun are indicative of the relationship between irradiance and temperature. The low amount of irradiance (Table 3) is coupled with the temperatures ranging between 29-34°C for the front and back sides of the module, while the ambient temperatures range primarily at 27-28°C.

Figure 3 shows the I-V curves obtained at 0.5 sun, while Tables 5 and 6 summarize the measured and calculated quantities at these levels. Unlike the variation observed at 0.25 sun, the irradiance are accompanied with similar temperature shifts ranging from 36-38°C for T_F, 34-35°C for T_B, and 28-31°C for T_A.

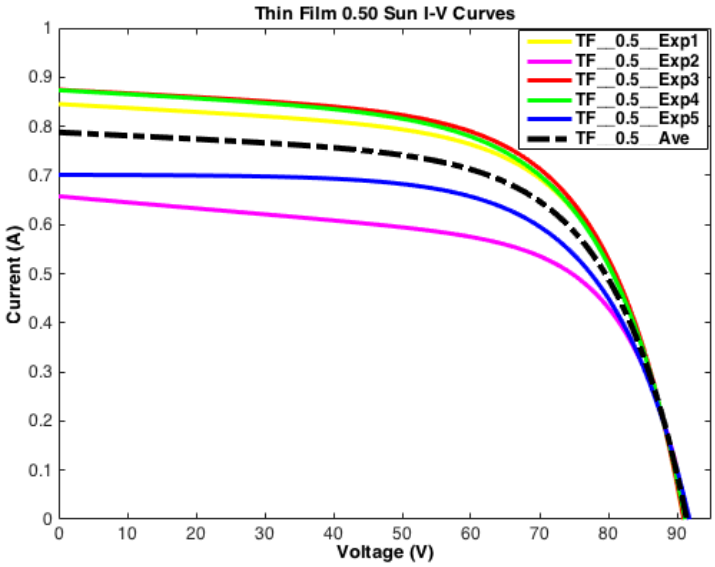

Figure 3. I-V curves at 0.5 sun.

Table 5. Environmental quantities at each 0.5 Sun I-V curve.

#	Curve Label	G_{ave} (W/m^2)	$T_{F(ave)}$ (°C)	$T_{B(ave)}$ (°C)	$T_{A(ave)}$ (°C)
6	TF_0.5_Exp1	531.771	36.9061	35.2229	29.9235
7	TF_0.5_Exp2	479.726	36.6017	34.0254	31.7898
8	TF_0.5_Exp3	543.698	38.0048	35.155	28.2814
9	TF_0.5_Exp4	542.554	37.7448	35.5063	27.9128
10	TF_0.5_Exp5	498.967	36.3878	35.6142	31.6966

Table 6. Electrical quantities at each 0.5 Sun I-V Curve.

#	Curve Label	P_{max} (W)	V_{MP} (V)	I_{MP} (A)	V_{OC} (V)	I_{SC} (A)	FF	η (%)
6	TF_0.5_Exp1	48.5904	69.7125	0.6970	90.9583	0.8454	0.6319	6.4303
7	TF_0.5_Exp2	37.6287	72.1875	0.5213	91.6668	0.6576	0.6242	5.5199
8	TF_0.5_Exp3	49.9917	69.3	0.7214	90.982	0.8744	0.6283	6.4706
9	TF_0.5_Exp4	49.0854	68.8875	0.7125	91.1783	0.8736	0.6162	6.3667
10	TF_0.5_Exp5	41.7246	69.3	0.6021	91.8105	0.7012	0.6481	5.8847

Figure 4 shows the I-V curves at 0.75 sun, accompanied by the quantities summarized in Tables 7 and 8.

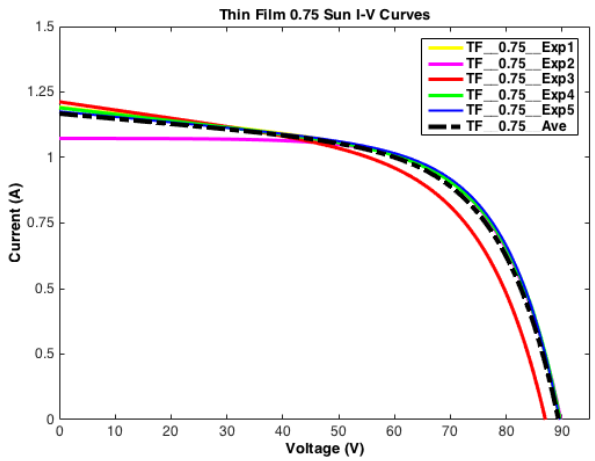

Figure 4. I-V curves at 0.75 sun

Consistent with the previous irradiance levels, the temperature measurements continue to increase at the module, in particular, above 40°C with 3-4°C higher than those obtained at 0.5 sun. The computed electrical quantities, meanwhile, begin to be more consistent, with efficiency staying close to 6 percent. A notable observation among the set is Curve 13, the increased ambient temperature offsets the decrease in measured front and back temperature to drop the power, fill factor and efficiency.

Figure 5 shows the plot of the I-V curves determined at 1 sun. As the irradiance is maximum at these curves, the short-circuit currents are also higher than any of the previous three sets of data. The open-circuit voltages are not as influenced by irradiance.

Table 7. Environmental quantities at each 0.75 sun I-V curve

#	Curve Label	G_{ave} (W/m^2)	$T_{F(ave)}$ (°C)	$T_{B(ave)}$ (°C)	$T_{A(ave)}$ (°C)
11	TF_0.75_Exp1	737.038	44.6406	42.0445	31.133
12	TF_0.75_Exp2	711.736	44.6232	42.5823	28.3975
13	TF_0.75_Exp3	721.435	42.6249	40.4565	32.4533
14	TF_0.75_Exp4	737.578	44.384	42.0012	30.0739
15	TF_0.75_Exp5	739.987	44.4253	42.092	30.3712

Table 8. Electrical quantities at each 0.75 Sun I-V Curve.

#	Curve Label	P_{max} (W)	V_{MP} (V)	I_{MP} (A)	V_{OC} (V)	I_{SC} (A)	FF	η (%)
11	TF_0.75_Exp1	63.7839	68.8875	0.9259	89.541	1.1929	0.5972	6.0902
12	TF_0.75_Exp2	63.8618	68.475	0.9326	89.7432	1.0728	0.6633	6.3144
13	TF_0.75_Exp3	58.5175	64.7625	0.9036	86.9944	1.2127	0.5547	5.7081
14	TF_0.75_Exp4	63.6483	68.8875	0.9239	89.6147	1.1899	0.5969	6.0727
15	TF_0.75_Exp5	64.373	68.8875	0.9345	89.521	1.1759	0.6115	6.1219

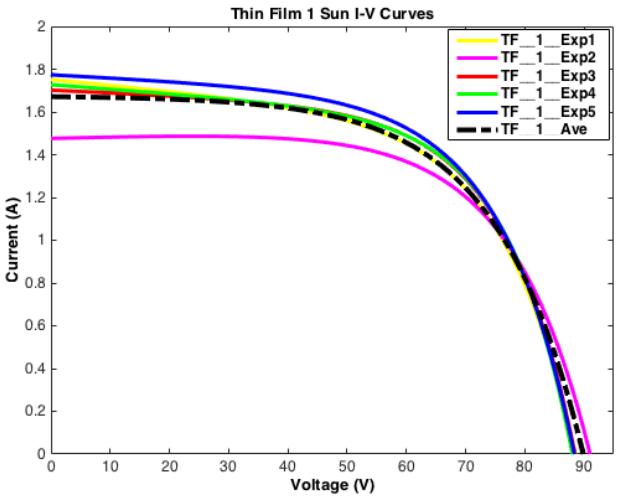

Figure 5. I-V curves at 1 sun

Tables 9 and 10 summarize the same environmental and electrical quantities during the data collection for 1 Sun I-V curves.

For 1 sun, the temperatures recorded at the front and back of the modules are mostly over 50°C, with ambient temperature also peaking at a higher value. At these values, however, the high irradiance is enough to increase maximum power. The high temperature influenced the decrease in voltage quantities such that the fill factor and efficiency still remain close to the values at 0.75 sun (Table 8).

Figure 6 shows the average I-V curves (#s 21-24) on the same plot.

For each of the four ranges of irradiance, the average curve represents the expected current-voltage characteristics exhibited by PV modules. On one hand, the short-circuit current I_{SC}, occurring at zero voltage, is also the maximum value found in the curve. On the other hand, the open-circuit voltage V_{OC} occurs at the rightmost part of each curve, where the current is zero. The shapes of all four curves are concave, facing downwards, with the maximum power point being the vertex of the concavity of the I-V curve.

Table 9. Environmental quantities at each 1 Sun I-V curve.

#	Curve Label	G_{ave} (W/m^2)	$T_{F(ave)}$ (°C)	$T_{B(ave)}$ (°C)	$T_{A(ave)}$ (°C)
16	TF_1_Exp1	1019.49	52.453	51.893	36.8584
17	TF_1_Exp2	926.262	43.0035	42.3649	32.3468
18	TF_1_Exp3	1041.68	51.1128	51.1677	38.6981
19	TF_1_Exp4	1051.45	51.4229	51.5907	33.7672
20	TF_1_Exp5	1083.05	52.8349	51.5837	32.8028

Table 10. Electrical quantities at each 1 Sun I-V curve.

#	Curve Label	P_{max} (°C)	V_{MP} (V)	I_{MP} (A)	V_{OC} (V)	I_{SC} (A)	FF	η (%)
16	TF_1_Exp1	88.7377	65.175	1.3615	88.5518	1.7519	0.572	6.1254
17	TF_1_Exp2	84.8484	66.825	1.2697	91.0105	1.476	0.6316	6.4463
18	TF_1_Exp3	91.5805	66	1.3875	88.4686	1.7021	0.6081	6.1869
19	TF_1_Exp4	91.7837	66	1.3907	88.0144	1.7275	0.6037	6.143
20	TF_1_Exp5	93.2162	65.175	1.4302	88.3839	1.7767	0.5936	6.057

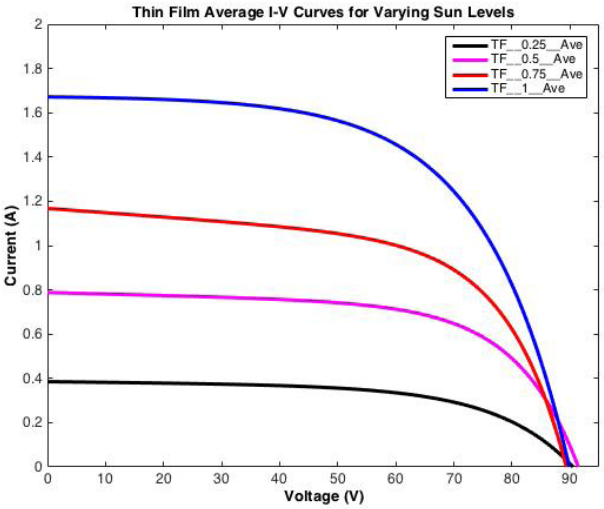

Figure 6. Comparison of average I-V curves at varying irradiance

It is observed that the vertical shifts are in direct proportion to the amount of irradiance available, in line with previously established trends; doubling the amount of irradiance from 0.25 sun (250 W/m^2) to 0.5 sun (500 W/m^2) shifts the current upwards twice. Similarly, the currents observed at 0.75 sun (750 W/m^2) and 1.00 sun (1000 W/m^2) are 3 and 4 times greater than the average, measured at 250 W/m^2 irradiance. This is emphasized by the shift in the short-circuit current. In terms of the open-circuit voltage, the I-V curves do not indicate any consistent shift. This supports the concept that the voltage is minimally influenced by irradiance.

In terms of electrical output as shown in Tables 4, 6, 8, and 10, the upward trend of power with irradiance was consistently observed; this is also reinforced by the response-to-irradiance behaviour of current (direct proportionality) and voltage (relatively indifferent). The fill factor and efficiency relationships do not exhibit the same near-linear proportionality. This is also supported by reviewing their respective formulas: fill factor compares current and voltage at the maximum power point relative to I_{SC} and V_{OC}, and thus the quantities experience similar shifts with irradiance. In the same manner, the efficiency is not proportional to irradiance, with the values ranging very close to 6%, as the reduction in input irradiance naturally reduces the available output power.

Statistical Analysis - Correlation

Using the twenty developed I-V curves, statistical analysis was done to arrive at the mathematical models for maximum power, fill factor, and efficiency.

The correlation among the four environmental parameters was first determined using Pearson's correlation coefficient. The *r*-statistic indicates the correlation between any pair of parameters, with the level of significance selected at $\alpha = 0.01$ (1%); that is, the *r*-statistic would be significant for $p < 0.01$.

The values of Table 11 show that there is a "strong" to "very strong" linear relationship between any pair of environmental variables,

Table 11. Pearson's correlation coefficient among the four environmental parameters.

a-Si Thin-Film					
	statistic	**T_F**	**T_B**	**T_A**	**G**
T_F	r	1	0.99356	0.7562	0.97537
	p		<.0001	0.0001	<.0001
T_B	r	0.99356	1	0.79183	0.97336
	p	<.0001		<.0001	<.0001
T_A	r	0.7562	0.79183	1	0.75046
	p	0.0001	<.0001		0.0001
G	r	0.97537	0.97336	0.75046	1
	p	<.0001	<.0001	0.0001	

coming to the conclusion of multicollinearity – and the need to perform factor analysis to arrive at the equations.

Factor Analysis and Regression

The results of the factor analysis are summarized in Table 12. The *factor* variable is interpreted as 'how much (in percent) of the electrical parameter's change' is explained by each corresponding environmental parameter.

Table 12. Loading factors calculated using factor analysis.

Parameter	Factor
$\mathbf{T_F}$	0.9906
$\mathbf{T_B}$	0.9982
$\mathbf{T_A}$	0.7945
G	0.9733

The results of the factor analysis reveal that for the particular thin-film module used, the front and back temperatures influence the output the most, with the irradiance not far behind. Furthermore, the ambient temperature, while it still accounts for 79% of the changes, falls as the least influential parameter.

The last step is to incorporate the factor loadings into the regression model, resulting in the following mathematical models in the form of Equation 4.

$$P_{MAX}(T_F,T_B,T_A,G) = -6.07353 + 0.08505(0.9906T_F + 0.9982T_B + 0.7945T_A + 0.9733G)$$

$$FF(T_F,T_B,T_A,G) = 0.65265 - (4.87E-05)(0.9906T_F + 0.9982T_B + 0.7945T_A + 0.9733G)$$

$$\eta_{MAX}(T_F,T_B,T_A,G) = 6.13737 - (2.29E-06)(0.9906T_F + 0.9982T_B + 0.7945T_A + 0.9733G)$$

Considering these equations, it is possible to estimate the output of the SF100 panel given a particular combination of environmental parameters. As an illustration, Table 13 shows the estimated maximum power while holding either of the three temperatures constant and varying the irradiance level:

Table 13. Model-estimated maximum power for varying environmental conditions.

G (W/m²)	T_F & T_B		T_B & T_A		T_F & T_A	
	min	max	min	max	min	Max
250	20.54	25.61	20.2	24.1	20.2	24.08
500	41.23	46.31	40.9	44.79	40.9	44.78
750	61.93	67	61.59	65.49	61.59	65.47
1000	82.62	87.7	82.29	86.18	82.29	86.16
	Ta = 25		Tf = 25		Tb = 25	

The results of Table 13 were estimated with the minimum possible temperature of 25°C and the maximum temperature of 60°C for T_F, T_B, and 40° for T_A, respectively. However, it must be noted that other environmental parameters such as wind speed and AM value were not incorporated in this model, which may still have influenced the output outside the boundaries considered in this study.

Conclusion

This study presented a method of characterizing the performance of a-Si photovoltaic modules with respect to irradiance and three temperatures: front/surface, back, and ambient temperatures. Using these measurements and the aid of curve fitting tools, acceptable I-V curves were modelled for various irradiance levels and used to calculate electrical quantities relevant to PV module performance; namely, maximum power, fill factor, and irradiance.

Similar trends in previous work were observed, with irradiance heavily influencing the amount of current available and, in turn, the maximum output power. Increasing the temperature also reveals a minimal change in the available voltage, but these changes are significantly offset by the influence of irradiance in output current. In particular, the shifts in the I-V curves show this direct proportionality of current to irradiance. The fill factor was relatively consistent at the different irradiance levels; this is explained by the similar changes in voltage and current at the fill factor calculation. The efficiency measurements are also relatively similar, at around 6%. As a comparison between input and output, a smaller irradiance naturally reduces the input power, and consequently the available output power.

Comparing the environmental parameters, there is a direct relationship between the irradiance ranges and the measured temperatures: temperatures obtained continued to increase as the irradiance increased; and, from 0.25 sun to 1 sun, temperatures at the surface increased by as much as 20oC. Furthermore, a strong correlation between these environmental parameters required the use of factor analysis in the regression process.

The results of this study showed the significant influence of irradiance, front/surface, and backside temperatures to the electrical performance of a-Si thin-film PV modules. In particular, the surface, backside temperatures, and irradiance mean much more for the performance (97-99%) than ambient temperature.

The model developed for maximum power supports the trends presented by the I-V characteristics. Specifically, proportional increase of the irradiance and the maximum power of the PV module would result despite the increase in the module temperatures (based from measurements). It is also revealed that this power is predicted to be higher if the associated increase in temperature with irradiance is addressed. The findings of this model prompt further studies that can focus more on the management and reduction of surface and backside temperatures that occur during higher irradiance conditions.
While the study was able to arrive at respectable models to estimate the performance of a PV module, it must be noted that several other factors, such as air mass, wind speed, and humidity were not incorporated in this work – these are also part of the assumptions of module ratings such as STP and NOCT. The effects of these environmental parameters to PV module performance are also worth considering for future study, as models can also be developed incorporating different environmental conditions using the same methods.

Finally, it is recommended to further increase the amount of I-V curves for characterization; this will allow for a refinement of the derived models. While the study aimed to consider four irradiance ranges, a particular focus on modeling the performance at only one level of irradiance (e.g., the lowest – 250 W/m^2) may also be considered.

Acknowledgments

The authors would like to recognize the financial support provided by the Commission on Higher Education (CHED), through its Faculty Development Program.

References

[1] S. A. Kalogirou, Solar Energy Engineering: Processes and Systems, Elsevier, Inc. , 2009.

[2] M. Fouad, L. Shihata and E. Morgan, "An Integrated Review of Factors Influencing the Performance of Photovoltaic Panels," *Renewable and Sustainable Energy Reviews,* vol. 80, pp. 1499-1511, 2017.

[3] R. Krishan, Y. Sood and B. Kumar, "The Simulation and Design for Analysis of Photovoltaic System Based on MATLAB," in *International Conference on Energy Efficient Technologes for Sustainability*, Nagercoil, India, 2013.

[4] A. Chouder, S. Silvestre, B. Taghezouit and E. Karatepe, "Monitoring, Modelling and Simulation of PV Systems Using LabVIEW," *Solar Energy,* vol. 91, pp. 337-349, 2013.

[5] E. Skoplaki and J. Palyvos, "On the Temperature Dependence of Photovoltaic Module Electrical Performance: A Review of Efficiency/Power Correlations," *Solar Energy,* vol. 83, pp. 614-624, 2009.

[6] F. M. Vanek, L. D. Albright and L. T. Angenent, Energy Systems Engineering: Evaluation and Implementation, 2nd Ed., McGraw-Hill, 2012.

[7] S. Dubey, J. Sarvaiya and B. Seshadri, "Temperature Dependent Photovoltaic (PV) Efficiency and its Effect on PV Production in the World - A review," *Energy Procedia,* vol. 33, pp. 311-321, 2013.

[8] E. Saloux, A. Teyssedou and M. Sorin, "Explicit Model of Photovoltaic Panels to Determine Voltages and Currents at the Maximum Power Point," *Solar Energy,* vol. 85, pp. 713-722, 2011.

[9] M. Park and I. Yu, "A Study on the Parameter Evaluation Method of Solar Cell," in *Annual Conference of IEEE Industrial Electronics Society*, Busan, Korea, 2004.

[10] R. Miceli, A. Orioli and A. Di Gangi, "A Procedure to Calculate the I-V Characteristics of Thin-Film Photovoltaic Modules Using an Explicit Rational Form," *Applied Energy,* vol. 155, pp. 613-628, 2015.

[11] S. Pindado and J. Cubas, "Simple Mathematical Approach to Solar Cell/ Panel Behavior Based on Datasheet Information," *Renewable Energy,* vol. 103, pp. 729-738, 2017.

[12] M. Hasan and S. Parida, "An Overview of Solar Photovoltaic Panel Modeling Based on Analytical and Experimental Viewpoint," *Renewable and Sustainable Energy Reviews,* vol. 30, pp. 75-83, 2016.

[13] N. Boutana, A. Melli, S. Haddad, A. Rabhi and A. Massi Pavan, "An Explicit I-V Model for Photovoltaic Module Technologies," *Energy Conversion and Management,* vol. 138, pp. 400-412, 2017.

[14] A. Alqahtani, M. Abuhamdeh and Y. Alsmadi, "A Simplified and Comprehensive Approach to Characterize Photovoltaic System Performance," in *IEEE Energytech 2012*, Cleveland, Ohio, 2012.

[15] A. Gxasheka, E. Van Dyk and E. Meyer, "Evaluation of Performance Parameters of PV Modules Deployed Outdoors," *Renewable Energy,* vol. 30, pp. 611-620, 2005.

[16] S. Rehman and I. El-Amin, "Performance Evaluation of an Off-Grid Photovoltaic System in Saudi Arabia," *Energy,* vol. 46, pp. 451-458, 2012.

[17] B. Verhelst, D. Caes, L. Vandevelde and J. Desmet, "Prediction of Yield of Solar Modules as a Function of Technologial and Climactic Parameters," in *International Conference on Clean Electrical Power (ICCEP)*, Alghero, 2013.

[18] S. Nizetic, F. Grubisic-Cabo, I. Marinic-Kragic and A. Papadopoulos, "Experimental and Numerical Investigation of a Backside Convective Cooling Mechanicsm on Photovoltaic Panels," *Energy,* vol. 111, pp. 211-225, 2016.

[19] T. Kozak, W. Maranda, A. Napieralski, G. De Man and A. De Vos, "Influence of Ambient Temperature on the Amount of Electric Energy Produced by Solar Modules," in *16th International Conference on Mixed Design of Integrated Circuits and Systems (MIXDES)*, Poland, 2009.

[20] R. Eke, T. Betts and R. Gottschalg, "Spectral Irradiance Effects on the Outdoor Performance of Photovoltaic Modules," *Renewable and Sustainable Energy Reviews,* vol. 69, pp. 429-434, 2017.
[21] A. C. Rencher, Methods of Multivariate Analysis, 2nd. Ed., John Wiley & Sons, Inc. , 2002.